

# Endo-4DGS: Distilling Depth Ranking for Endoscopic Monocular Scene Reconstruction with 4D Gaussian Splatting

Yiming Huang<sup>1</sup> \*, Beilei Cui<sup>1</sup> \*, Long Bai<sup>1</sup> \*, Ziqi Guo<sup>1</sup>, Mengya Xu<sup>1</sup>, and Hongliang Ren<sup>1,2,3</sup> \*\*

<sup>1</sup> Department of Electronic Engineering, The Chinese University of Hong Kong (CUHK), Hong Kong SAR, China

<sup>2</sup> Shun Hing Institute of Advanced Engineering, CUHK, Hong Kong SAR, China

<sup>3</sup> Shenzhen Research Institute, CUHK, Shenzhen, China

{yhuangdl, beileicui, b.long}@link.cuhk.edu.hk, hlren@ee.cuhk.edu.hk

**Abstract.** In the realm of robot-assisted minimally invasive surgery, dynamic scene reconstruction can significantly enhance downstream tasks and improve surgical outcomes. Neural Radiance Fields (NeRF)-based methods have recently risen to prominence for their exceptional ability to reconstruct scenes. Nonetheless, these methods are hampered by slow inference, prolonged training, and substantial computational demands. Additionally, some rely on stereo depth estimation, which is often infeasible due to the high costs and logistical challenges associated with stereo cameras. Moreover, the monocular reconstruction quality for deformable scenes is currently inadequate. To overcome these obstacles, we present Endo-4DGS, an innovative, real-time endoscopic dynamic reconstruction approach that utilizes 4D Gaussian Splatting (GS) and requires no ground truth depth data. This method extends 3D GS by incorporating a temporal component and leverages a lightweight MLP to capture temporal Gaussian deformations. This effectively facilitates the reconstruction of dynamic surgical scenes with variable conditions. We also integrate Depth-Anything to generate pseudo-depth maps from monocular views, enhancing the depth-guided reconstruction process. Our approach has been validated on two surgical datasets, where it has proven to render in real-time, compute efficiently, and reconstruct with remarkable accuracy. These results underline the vast potential of Endo-4DGS to improve surgical assistance.

## 1 Introduction

Endoscopic procedures have become a cornerstone in minimally invasive surgery, offering patients with reduced trauma and quicker recovery times [8, 16, 27]. In this case, accurate and dynamic 3D reconstruction of the endoscopic scene is

---

\* Co-first authors.

\*\* Corresponding author.

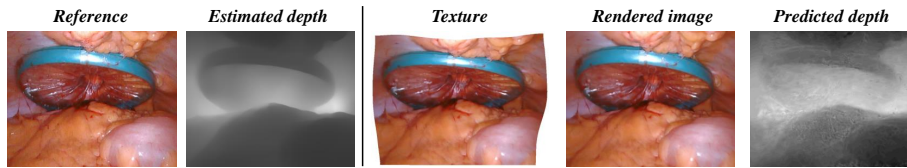


**Fig. 1.** 3D textures, rendered image, and predicted depth of our proposed method.

critical to enhancing the surgeon’s spatial understanding and navigation, facilitating more precise and efficient interventions [13]. However, the complex and constrained nature of endoscopic scenes poses significant challenges for traditional 3D reconstruction techniques due to factors such as limited field-of-view, occlusions, and dynamic tissue deformation [20, 23, 26].

Recent advancements in endoscopic 3D reconstruction have been boosted by the capabilities of Deep Neural Networks (DNNs) [19] and Neural Radiance Fields (NeRFs) [14]. Some studies have achieved strong performance in depth estimation and reconstruction under endoscopy, particularly through stereo reconstruction [2, 12], structure from motion [3], depth and pose estimation [15, 18] or extensive visual pre-training [6]. However, reconstructing high-dimensional deformable scenes remains a challenge. EndoNeRF [20] marks a significant step forward, being the first to leverage NeRF’s ability for implicit geometric modeling in endoscopic scenes. It introduces a dual neural field approach to model tissue deformation and canonical density, achieving dynamic scene rendering and the removal of instrument occlusion during endoscopic-assisted surgery. Building on this, EndoSurf [26] further employs signed distance functions to model tissue surfaces, imposing explicit self-consistency constraints on the neural field. To tackle the real-time dynamic reconstruction challenge, LerPlane [23] constructs a 4D volume by introducing 1D time to the existing 3D spatial space. This extension allows for the formulation of both static fields and dynamic fields by utilizing the spatial and spatiotemporal planes, respectively, which leads to a substantial decrease in computational resources.

NeRF-based methods are transformative in 3D scene reconstruction but struggle with slow rendering and less-than-ideal localization accuracy [5]. To circumvent these limitations, 3D Gaussian Splatting (GS) has emerged as a promising technique, celebrated for its fast inference and high-quality 3D representation learning [10]. 3D GS uses a collection of scene images to optimize anisotropic 3D Gaussians, capturing their positions, orientations, appearances, and alpha blending parameters. This effectively reconstructs both the geometric structure and visual appearance of a scene. The tile-based rasterizer of 3D GS ensures rapid rendering.

Drawing inspiration from [21], we introduce the concept of time as the 4<sup>th</sup> dimension to model dynamic scenes, specifically targeting the reconstruction challenges of deformable tissues in endoscopic surgery. Traditional methods typically rely on multi-view reconstruction, which is often impractical in vivo, given the

prohibitive costs and size constraints of stereo cameras in endoscope-assisted procedures. Furthermore, amassing a comprehensive, fully supervised depth dataset is not feasible [18]. Depth-Anything [24], a novel technique with extensive visual pre-training, has shown exceptional depth estimation performance in diverse scenes. We harness Depth-Anything [24] to estimate depth maps from monocular cameras, guiding and refining our 3D reconstruction. Figure 1 presents the 3D textures, rendered images, and predicted depth in endoscopic views. Specifically, our contributions in this paper are threefold:

- We present Endo-4DGS, an innovative technique that adapts Gaussian Splatting for endoscopic scene reconstruction. Utilizing Depth-Anything, Endo-4DGS achieves remarkable reconstruction outcomes without needing ground truth depth data.
- We use a lightweight MLP to predict the temporal dynamics of deformable tissues, creating a 4D voxel model for dynamic scenes. Depth-Anything aids in estimating depth from a single camera viewpoint, acting as pseudo-depth supervision for convergence.
- Our extensive validation on two real surgical datasets shows that Endo-4DGS attains high-quality reconstruction, excels in real-time performance, reduces training expenditures, and demands less GPU memory, which sets the stage for advancements in robot-assisted surgery.

## 2 Methodology

In this section, we introduce the representation and rendering formula of 4D Gaussians [21] in Sec. 2.1 and demonstrate our motivation and detailed implementation of the depth prior-based reconstruction in Sec. 2.2.

### 2.1 Preliminaries

3D GS [10] utilizes 3D differentiable Gaussians as the unstructured representation, allowing for a differentiable volumetric representation that can be rapidly rasterized and projected onto a 2D surface for swift rendering. With a covariance matrix  $\Sigma$  and a center point  $\mathcal{X}$ , we can represent the 3D Gaussians as following:

$$G(X) = e^{-\frac{1}{2}\mathcal{X}^T \Sigma^{-1} \mathcal{X}}, \quad (1)$$

where the covariance  $\Sigma$  can be further decomposed into  $\Sigma = \mathbf{R}\mathbf{S}\mathbf{S}^T\mathbf{R}^T$ , which includes a scaling  $\mathbf{S}$  and rotation  $\mathbf{R}$ . With the differential splatting rendering method [25], 3D Gaussians [10] achieves real-time rendering for photo-realistic results.

### 2.2 Proposed Methodology

**Overview of the Endo-4DGS Pipeline.** The whole pipeline of Endo-4DGS is illustrated in Figure 2. The Endo-4DGS method consists of four major parts,

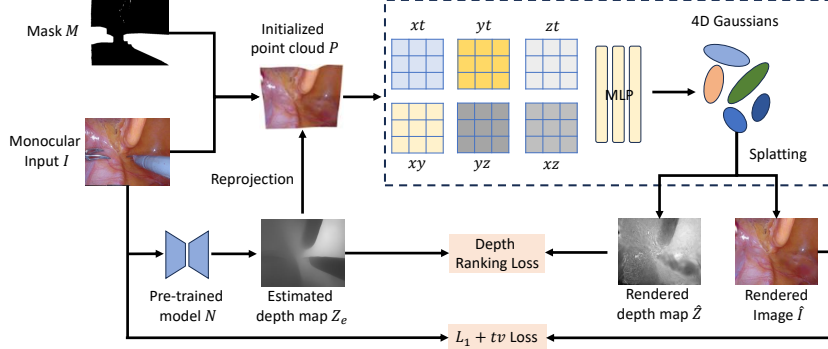


Fig. 2. Illustration of our proposed Endo-4DGS framework.

i.e. the depth estimation module, the depth initialization module, the color reconstruction module, and the depth ranking distilling module. We employ 4D Gaussians as the backbone for 4D scene reconstruction and utilize the Depth-Anything [24] model pre-trained on 63.5M images to estimate the depth map from monocular input. The training data of Depth-Anything [24] covers a wide range of data, therefore it is robust on the relative distance for estimated depth map which can provide the geometry guidance with our depth ranking distilling module. With the implementation of the depth prior, we address the initialization and depth supervision problem under monocular scene reconstruction.

**4D Gaussian Splatting** Inspired by [21], the static representation of 3D GS [10] shall be extended to 4D by constructing a new Gaussian representation with motions and shape deformations. Given the differential splatting rendering formula  $\mathcal{S}$ , 4D Gaussians representation  $\mathcal{G}'$ , and the camera extrinsic matrix  $K_2 = [R, T]$ , the novel-view image  $\hat{I}$  can be rendered as:

$$\hat{I} = \mathcal{S}(K_2, \mathcal{G}'), \quad (2)$$

where the 4D Gaussians is formed as  $\mathcal{G}' = \Delta\mathcal{G} + \mathcal{G}$  by a static 3D Gaussians  $\mathcal{G}$  and its deformation  $\Delta\mathcal{G}$ . With the deformation function  $\mathcal{F}$  and time  $t$ , the deformation can be described as  $\Delta\mathcal{G} = \mathcal{F}(\mathcal{G}, t)$ .

More specifically, a multi-resolution HexPlane voxel module  $R(I, j) \in \mathbb{R}^{h \times l N_i \times l N_j}$  is utilized, where  $h$  is the hidden dim of features,  $N$  is the resolution of the voxel grids and  $l$  is the upsampling scale. With a tiny MLP  $\phi_d$ , the voxel features  $f_h \in \mathbb{R}^{h * l}$  of time  $t$  is encoded as temporal and spatial features  $f_d$ :

$$\begin{aligned} f_d &= \phi_d(f_h) \\ f_h &= \bigcup_l \prod \text{interp}(R(i, j)), \\ \{i, j\} &\in \{(x, y), (x, z), (y, z), (x, t), (y, t), (z, t)\}. \end{aligned} \quad (3)$$

In addition, a multi-head Gaussian deformation decoder  $\mathcal{D} = \{\phi_x, \phi_r, \phi_s\}$  is designed for decoding the deformation of position, rotation, and scaling of the 3D Gaussians with three tiny MLPs:  $\phi_x, \phi_r, \phi_s$ , respectively. With the deformation of position  $\Delta\mathcal{X} = \phi_x(f_d)$ , rotation  $\Delta r = \phi_r(f_d)$ , and scaling  $\Delta s = \phi_s(f_d)$ , the final representation of 4D Gaussians can be presented as:

$$\mathcal{G}' = \{\mathcal{X} + \Delta\mathcal{X}, r + \Delta r, s + \Delta s, \sigma, \mathcal{C}\}, \quad (4)$$

where  $\mathcal{X}, r, s$  are the original position, rotation, and scaling of the static 3D Gaussian representation, while  $\sigma$  is the density and  $\mathcal{C}$  is the color.

**Gaussians Initialization with Depth Prior.** Previous work [10] has demonstrated the importance of applying point cloud from Shape from Motion (SfM) [17] as an initialization for the 3D Gaussians. However, retrieving accurate point clouds in surgical scenes is challenging due to the hardware constraints and the varying illumination conditions. Existing solutions includes generating sparse 3D points by COLMAP [17] or using Multi-View Stereo (MVS) algorithms [1, 9, 11]. However, in real-world applications, the only visual information from the consumer-level endoscopes is the monocular RGB image. With such a limitation, we propose to use the pre-trained depth to implement the point cloud initialization for the 4D Gaussians. With the pre-trained depth estimation model  $\mathcal{N}$  and the input image  $I_0$  of width  $W$  and height  $H$ , we estimate an inversed depth map  $Z_e \in \mathbb{R}^{H \times W}$ . Then we apply a scaling  $\alpha$  to convert the estimated inverse depth to the depth map  $Z_c$  in the camera coordinate as  $Z_c = \frac{\alpha}{Z_e}$ . Given the camera intrinsic matrix  $K_1$ , and the extrinsic matrix  $K_2$ , we can reproject the point cloud  $P_0 \in \mathbb{R}^{HW \times 3}$  for initialization from the given image  $I_0$  as follows:

$$P_0 = Z_c K_2^{-1} K_1^{-1} (I_0 \odot M_0), \quad (5)$$

where  $M_0$  is the mask for the input image, and  $\odot$  is the element-wise multiplication. with the initialized point cloud from the pre-train depth map, the training process of the 4D-GS can be more robust in terms of geometry.

**Distilling Depth Ranking and Optimization.** Single-image depth estimation is a challenging task due to the ill-pose nature and the bias from various datasets. To utilize the pre-train depth map more effectively as the pseudo-ground truth, we propose to use a structure-guided ranking loss [22]  $\mathcal{L}_{rk}$ . With the depth distilling loss, we enable the constraint for the rendered depth without knowing the shift and scale. With the  $\mathcal{L}_1$  color loss and a grid-based total-variational loss  $\mathcal{L}_{tv}$  [4, 7], our final loss for optimizing can be represented as:

$$\mathcal{L} = \mathcal{L}_1 + \mathcal{L}_{tv} + \lambda \mathcal{L}_{rk}, \quad (6)$$

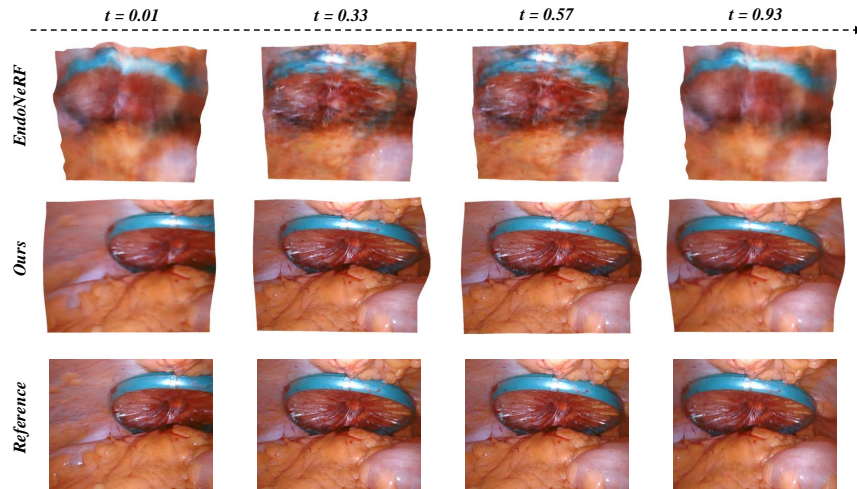
where  $\lambda$  is the weight for the depth ranking loss.

**Table 1.** Comparison experiments on the EndoNeRF dataset [20] against EndoNeRF [20], EndoSurf [26], and LerPlane [23].

Models	EndoNeRF-Cutting			EndoNeRF-Pulling			Training	FPS	GPU
	PSNR	SSIM	LPIPS	PSNR	SSIM	LPIPS	Time		Usage
EndoNeRF [20]	35.84	0.942	0.057	35.43	0.939	0.064	6 hours	0.2	4 GB
EndoSurf [26]	34.89	0.952	0.107	34.91	0.955	0.120	7 hours	0.04	17 GB
LerPlane [23]	34.66	0.923	0.071	31.77	0.910	0.071	8 mins	1.5	20 GB
Ours	<b>36.84</b>	<b>0.954</b>	<b>0.040</b>	<b>37.08</b>	<b>0.955</b>	<b>0.050</b>	<b>4 mins</b>	<b>100</b>	<b>4GB</b>

**Table 2.** Comparison experiments on the StereoMIS dataset [9] against EndoNeRF [20].

Models	PSNR	SSIM	LPIPS	Training	FPS	GPU
				Time		Usage
EndoNeRF [20]	21.49	0.622	0.360	5 hours	0.2	4 GB
Ours	<b>31.46</b>	<b>0.829</b>	<b>0.175</b>	<b>5 mins</b>	<b>100</b>	<b>4GB</b>

**Fig. 3.** Qualitative comparison on the StereoMIS dataset [9] against EndoNeRF [20].

### 3 Experiments

#### 3.1 Dataset

We evaluate the performance based on two publicly available datasets, StereoMIS [9] and EndoNeRF [20]. The StereoMIS dataset is a stereo video dataset captured by the da Vinci Xi surgical system, consisting of 11 surgical sequences by in-vivo porcine subjects. The EndoNeRF dataset includes two samples of prostatectomy via stereo cameras and provides estimated depth maps based on stereo-matching techniques, they also include challenging scenes with tool oc-

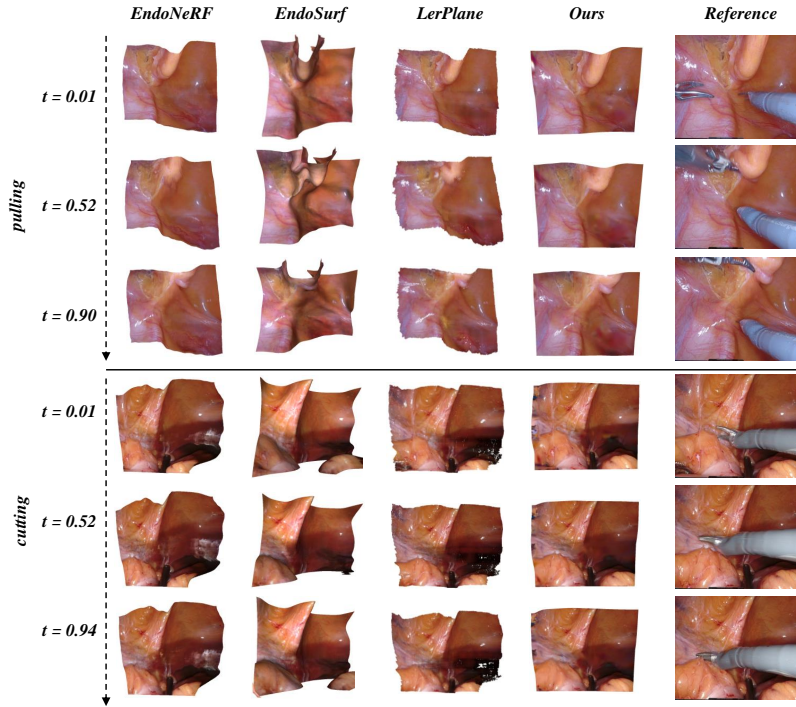


**Fig. 4.** Qualitative comparison on the EndoNeRF dataset [20] against EndoNeRF [20], EndoSurf [26], and LerPlane [23].

clusion and non-rigid deformation. The training and validation splitting follows the 7:1 strategy in [26]. We use PSNR, SSIM, and LPIPS to evaluate the 3D scene reconstruction performance. We also report the results of training time, inference speed, and GPU memory usage on one single RTX4090 GPU.

### 3.2 Implementation Details

All experiments are conducted on the RTX4090 GPU with the Python PyTorch framework. We adopt the Adam optimizer with an initial learning rate of  $1.6 \times 10^{-3}$ . We employ the Depth-Anything-Small model for pseudo-depth map generation with depth scale  $\alpha = 1000$  and  $\lambda = 0.01$  as the weight for the depth ranking loss. We use an encoding voxel size of [64, 64, 64, 75], where the four dimensions are length, width, height, and time, respectively.

### 3.3 Results

We compare the performance of our method against the state-of-the-art methods, e.g., EndoNeRF [20], EndoSurf [26], and LerPlane [23]. The evaluation performances on StereoMIS and EndoNeRF are shown in Table 2 and Table 1. We

can observe that while maintaining relatively high performance for EndoNeRF and EndoSurf, they both require hours of training which is time-consuming. LerPlane greatly reduces the training time to around 8 minutes at the cost of slight degradation in rendering performance. It is worth noting that all these state-of-the-art methods suffer from very low FPS which limits their further application in real-time surgical scene reconstruction tasks. Our proposed method not only achieves the best performance in all evaluation metrics on two datasets but also increases the inference speed to a real-time level of 100 FPS with only 4 minutes of training and 4G of GPU usage. We also illustrate some qualitative results for both datasets in Figure 3 and 4. It can be observed that for StereoMIS, EndoNeRF can not capture the details of tissues while our proposed method preserves a large amount of visible details with good geometry features. Our proposed method also rendered better visualizations of the EndoNeRF dataset compared to other methods. The above quantitative and qualitative results certificate that Endo-4DGS achieves high-quality 3d reconstruction scenes with real-time level inference speed which reveals its strong potential in future real-time endoscopic applications.

## 4 Conclusion

In conclusion, our study marks a substantial progression in robot-assisted surgery by offering an innovative and effective approach to dynamic scene reconstruction. Endo-4DGS harnesses 4D Gaussian Splatting and Depth-Anything, enabling the real-time, high-fidelity reconstruction of deformable tissues without relying on ground truth depth information. Our strategic application of a lightweight MLP for predicting deformable tissue dynamics, combined with Depth-Anything for monocular depth estimation, allows Endo-4DGS to outperform existing methods in accuracy and computational efficiency. The decreased GPU memory requirement and independence from extensive depth data are key achievements that promise wider application and further innovation in the domain. Furthermore, our work presents practical benefits, as it can be easily integrated into clinical practice to boost the surgeon’s spatial perception and decision-making during surgeries.

**Acknowledgements.** This work was supported by Hong Kong RGC Collaborative Research Fund (C4026-21G), General Research Fund (GRF 14211420 & 14203323), Shenzhen-Hong Kong-Macau Technology Research Programme (Type C) STIC Grant SGDX20210823103535014 (202108233000303).

## References

1. Allan, M., Mcleod, J., Wang, C., Rosenthal, J.C., Hu, Z., Gard, N., Eisert, P., Fu, K.X., Zeffiro, T., Xia, W., et al.: Stereo correspondence and reconstruction of endoscopic data challenge. arXiv preprint arXiv:2101.01133 (2021)

2. Bae, G., Budvytis, I., Yeung, C.K., Cipolla, R.: Deep multi-view stereo for dense 3d reconstruction from monocular endoscopic video. In: International Conference on Medical Image Computing and Computer-Assisted Intervention. pp. 774–783. Springer (2020)
3. Barbed, O.L., Montiel, J.M., Fua, P., Murillo, A.C.: Tracking adaptation to improve superpoint for 3d reconstruction in endoscopy. In: International Conference on Medical Image Computing and Computer-Assisted Intervention. pp. 583–593. Springer (2023)
4. Cao, A., Johnson, J.: Hexplane: A fast representation for dynamic scenes. In: Proceedings of the IEEE/CVF Conference on Computer Vision and Pattern Recognition. pp. 130–141 (2023)
5. Chen, G., Wang, W.: A survey on 3d gaussian splatting. arXiv preprint arXiv:2401.03890 (2024)
6. Cui, B., Islam, M., Bai, L., Ren, H.: Surgical-dino: Adapter learning of foundation model for depth estimation in endoscopic surgery. arXiv preprint arXiv:2401.06013 (2024)
7. Fang, J., Yi, T., Wang, X., Xie, L., Zhang, X., Liu, W., Nießner, M., Tian, Q.: Fast dynamic radiance fields with time-aware neural voxels. In: SIGGRAPH Asia 2022 Conference Papers. pp. 1–9 (2022)
8. Gao, H., Yang, X., Xiao, X., Zhu, X., Zhang, T., Hou, C., Liu, H., Meng, M.Q.H., Sun, L., Zuo, X., et al.: Transendoscopic flexible parallel continuum robotic mechanism for bimanual endoscopic submucosal dissection. *The International Journal of Robotics Research* p. 02783649231209338 (2023)
9. Hayoz, M., Hahne, C., Gallardo, M., Candinas, D., Kurmann, T., Allan, M., Sznitman, R.: Learning how to robustly estimate camera pose in endoscopic videos. *International Journal of Computer Assisted Radiology and Surgery* pp. 1185–1192 (2023)
10. Kerbl, B., Kopanas, G., Leimkühler, T., Drettakis, G.: 3d gaussian splatting for real-time radiance field rendering. *ACM Transactions on Graphics* **42**(4) (2023)
11. Li, Z., Liu, X., Drenkow, N., Ding, A., Creighton, F.X., Taylor, R.H., Unberath, M.: Revisiting stereo depth estimation from a sequence-to-sequence perspective with transformers. In: Proceedings of the IEEE/CVF international conference on computer vision. pp. 6197–6206 (2021)
12. Long, Y., Li, Z., Yee, C.H., Ng, C.F., Taylor, R.H., Unberath, M., Dou, Q.: E-dssr: efficient dynamic surgical scene reconstruction with transformer-based stereoscopic depth perception. In: Medical Image Computing and Computer Assisted Intervention–MICCAI 2021: 24th International Conference, Strasbourg, France, September 27–October 1, 2021, Proceedings, Part IV 24. pp. 415–425. Springer (2021)
13. Mahmoud, N., Cirauqui, I., Hostettler, A., Doignon, C., Soler, L., Marescaux, J., Montiel, J.M.M.: Orbslam-based endoscope tracking and 3d reconstruction. In: Computer-Assisted and Robotic Endoscopy: Third International Workshop, CARE 2016, Held in Conjunction with MICCAI 2016, Athens, Greece, October 17, 2016, Revised Selected Papers 3. pp. 72–83. Springer (2017)
14. Mildenhall, B., Srinivasan, P.P., Tancik, M., Barron, J.T., Ramamoorthi, R., Ng, R.: Nerf: Representing scenes as neural radiance fields for view synthesis. *Communications of the ACM* **65**(1), 99–106 (2021)
15. Ozyoruk, K.B., Gokceler, G.I., Bobrow, T.L., Coskun, G., Incetan, K., Almalioglu, Y., Mahmood, F., Curto, E., Perdigoto, L., Oliveira, M., et al.: Endoslam dataset and an unsupervised monocular visual odometry and depth estimation approach for endoscopic videos. *Medical image analysis* **71**, 102058 (2021)

16. Psychogyios, D., Colleoni, E., Van Amsterdam, B., Li, C.Y., Huang, S.Y., Li, Y., Jia, F., Zou, B., Wang, G., Liu, Y., et al.: Sar-rarp50: Segmentation of surgical instrumentation and action recognition on robot-assisted radical prostatectomy challenge. arXiv preprint arXiv:2401.00496 (2023)
17. Schonberger, J.L., Frahm, J.M.: Structure-from-motion revisited. In: Proceedings of the IEEE Conference on Computer Vision and Pattern Recognition (CVPR) (June 2016)
18. Shao, S., Pei, Z., Chen, W., Zhu, W., Wu, X., Sun, D., Zhang, B.: Self-supervised monocular depth and ego-motion estimation in endoscopy: Appearance flow to the rescue. *Medical image analysis* **77**, 102338 (2022)
19. Stucker, C., Schindler, K.: Resdepth: Learned residual stereo reconstruction. In: Proceedings of the IEEE/CVF Conference on Computer Vision and Pattern Recognition Workshops. pp. 184–185 (2020)
20. Wang, Y., Long, Y., Fan, S.H., Dou, Q.: Neural rendering for stereo 3d reconstruction of deformable tissues in robotic surgery. In: International Conference on Medical Image Computing and Computer-Assisted Intervention. pp. 431–441. Springer (2022)
21. Wu, G., Yi, T., Fang, J., Xie, L., Zhang, X., Wei, W., Liu, W., Tian, Q., Xinggang, W.: 4d gaussian splatting for real-time dynamic scene rendering. arXiv preprint arXiv:2310.08528 (2023)
22. Xian, K., Zhang, J., Wang, O., Mai, L., Lin, Z., Cao, Z.: Structure-guided ranking loss for single image depth prediction. In: Proceedings of the IEEE/CVF Conference on Computer Vision and Pattern Recognition. pp. 611–620 (2020)
23. Yang, C., Wang, K., Wang, Y., Yang, X., Shen, W.: Neural lerplane representations for fast 4d reconstruction of deformable tissues. arXiv preprint arXiv:2305.19906 (2023)
24. Yang, L., Kang, B., Huang, Z., Xu, X., Feng, J., Zhao, H.: Depth anything: Unleashing the power of large-scale unlabeled data. arXiv:2401.10891 (2024)
25. Yifan, W., Serena, F., Wu, S., Öztireli, C., Sorkine-Hornung, O.: Differentiable surface splatting for point-based geometry processing. *ACM Transactions on Graphics (TOG)* **38**(6), 1–14 (2019)
26. Zha, R., Cheng, X., Li, H., Harandi, M., Ge, Z.: Endosurf: Neural surface reconstruction of deformable tissues with stereo endoscope videos. In: International Conference on Medical Image Computing and Computer-Assisted Intervention. pp. 13–23. Springer (2023)
27. Zia, A., Bhattacharyya, K., Liu, X., Berniker, M., Wang, Z., Nespolo, R., Kondo, S., Kasai, S., Hirasawa, K., Liu, B., et al.: Surgical tool classification and localization: results and methods from the miccai 2022 surgtoolloc challenge. arXiv preprint arXiv:2305.07152 (2023)